Geoinformation for European-wide Integration, Benes (ed.)

Assessing the potential of hyperspectral angular imaging of urban built form surfaces for the inference of fine spatial scale urban land cover information

Louise Mackay & Stuart Barr
School of Geography, University of Leeds, Leeds, LS2 9JT, United Kingdom
l.mackay@geog.leeds.ac.uk

Keywords: hyperspectral, urban surface materials, angular reflectance, 3-Dimensional structure

ABSTRACT: The accurate and consistent extraction of man-made land cover types from high spatial resolution multispectral remotely-sensed images remains a significant barrier to the operational use of Earth observation for the mapping and monitoring of urban areas. In relation to this point, a number of recent studies have suggested that high spatial resolution hyperspectral data may allow the accurate derivation of man-made land cover types. Such studies have, however, been primarily applied in urban areas where building roofs are predominantly planimetric (flat) and the number of different man-made roof and road surface types is somewhat limited. Moreover, it would seem, to date, that no evaluation has been made on the potential discriminatory value of obtaining images of varying solar illumination and sensor viewing angle for different man-made land cover types. In this paper, we investigate the potential of multi-angular hyperspectral measurements of man-made objects in relation to the ability to improve the inference of urban land cover. This is achieved by analysing spectrometer reflectance measurements acquired for multiple illumination and viewing angles over a series of physically scaled 3-D roof-models of different material. The results obtained from this sampling show that multiple view angle measurements potentially allow different urban mad-made land cover types to be distinguished.

1 INTRODUCTION

In order to map and monitor urban change, and hence urban sustainability, information on land cover is required for both the physical-based analysis of the urban landscape as well as, the subsequent inference of urban land use. The use of low spatial and radiometric resolution satellite images has in the past, however, provided relatively poor information on urban land cover and land use (Sadler et al., 1991). In particular, previous remote sensing studies suggest that the classification of urban land cover from broadband multispectral images is problematic using traditional statistical spectral pattern recognition techniques (Heikkonen and Varfis, 1998), as many man-made land cover surfaces often exhibit a similar spectral response.

However, a number of recent studies have found for hyperspectral airborne images of urban scenes that many urban land cover types do exhibit a distinct spectral response (Ben Door et al., 2001; Roessner et al., 2001); results that are supported by laboratory-based spectroscopy measurements of man-made materials used in the construction of roads and roofs (Price, 1995). Many of these studies, however, have been conducted in urban areas where the underlying building-roof geometry is planimetric (*i.e.,* flat) and hence have failed to investigate the affect of built-form geometry and orientation (*e.g.,* gable-roof geometry) on the hyperspectral reflectance measurements obtained. Furthermore, in urban areas where gable-roofs dominate, such as in residential areas of western European cities, one may expect recorded reflectance to have an increased sensitivity to the underlying illumination and view angle of acquisition. It would seem, however, that such illumination/view angle effects have not been quantitatively investigated in relation to the discrimination of man-made objects using hyperspectral reflectance measurements.

In order to address these issues, this paper reports the results of a detailed hyperspectral sampling of urban land cover types consisting of composite surface materials. This is undertaken to characterise the relationships that exist between man-made built-form urban materials, built-form object geometry, and changes in the illumination and view angle geometry. These issues are analysed by quantifying the hyperspectral reflectance of a sample of urban surface materials.

2 METHODS

2.1 *Hyperspectral sampling of urban surface materials*

Hyperspectral reflectance measurements were acquired for a range of British roof and road surface materials (Table 1). Reflectance measurements were taken around solar noon using an Analytical Spectral Device's FieldSpec® Pro; a portable narrow band (1200 channels) visible (350μm) to short-wave near-infrared (2500μm) field spectrometer. The roof and road material samples were situated at a flat and unoccluded outdoor location. The reflectance measurements were taken with an 8^0 fore optic at nadir and for 15^0 changes in viewing zenith and azimuth angles.

Table 1. The roof and road surface materials used in the investigation

Surface material type	Approximate date of construction
Asphalt roof sheeting	2001
Black Cement roof tile	2001
Brown Cement roof tile	1930
Clay roof tile	1930
Red Cement roof tile	2001
Slate roof tile	1900
Tarmac road surfacing	1999

2.2 *Hyperspectral sampling of 3-dimensional roof geometry*

In order to obtain reflectance measurements relating to roof-geometry scaled gable-roof models were constructed that adhered to an average British roof-frame (internal apex angle of 37^0 from normal) (Smit & Chandler, 1991). Measurements were recorded for these individually and also in terms of a two roof-model configuration, such that one roof-model partially occluded direct solar illumination of the other (Figures 1 and 2). In both instances the roof faces were positioned perpendicular to the solar principal plane. During sampling, the time of day was recorded for each of the measurements taken in order to allow the subsequent solar azimuth and zenith angles to be calculated for the latitude of the field site.

2.3 *Narrowband to broadband conversion*

In order to provide a baseline comparison of the discriminatory power of the multiple view angle hyperspectral measurements taken, planimetric reflectance measurements for the different materials under investigation were converted to broadband reflectance values that corresponded to the 4 spectral bands of the very high spatial resolution IKONOS multispectral sensor (4m). This was achieved by using the individual spectral responsivity curves of the IKONOS bands (Space Imaging, 2002). Each of these were first converted from their original $3\,\eta m$ sampling interval to the $1\,\eta m$ frequency of the hyperspectral measurements by means of linear piecewise interpolation. The resulting curves were then convolved with the recorded hyperspectral measurements that fell within the bandwidth of each IKONOS band; in order to derive the band specific responsivity weighted numerically integrated broadband reflectance.

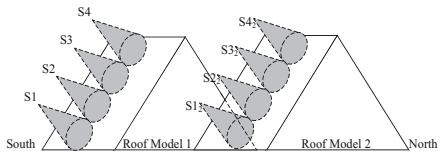

Figure 1. An illustration of the sampling strategy used for the two-roof neighbourhood experiment. The left-hand roof sensor fore optic positions (S1, S2, S3, and S4) are replicated for the obstructed right-hand roof ($S1_2$, $S2_2$, $S3_2$, and $S4_2$). During sampling the sensor fore optic was positioned normal to the roof surface and at intervals where the sensor instantaneous field of view (footprint) did not overlap. Both roof models were placed with the roof face perpendicular to the solar principal plane.

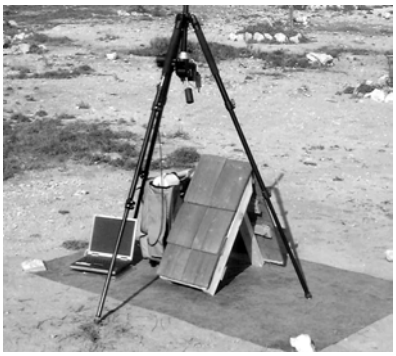

Figure 2. A photograph showing the spectrometer set-up and roof model used in the field. The roof tiles were placed on a slatted roof model, which allowed complete overlap of the sample surface material for accurate reflectance measurement.

3 RESULTS

3.1 *The reflectance of planimetric urban surface materials*

Figure 3 shows the recorded reflectance curves of the sample materials under investigation when placed in a planimetric manner (*i.e.*, flat). Interestingly, the black cement roof tile shows an unexpectedly high reflectance through most of the spectral range. According to United States Geological Survey laboratory spectroscopy measurements, quartz produces a similarly high reflectance, due to its crystal structural and vibrational characteristics (Clarke, 1999). Analysis of the black cement tile showed that

it contained a high level of quartz which is the most likely explanation for the high reflectance recorded for this roofing material. Figure 3 also shows that surfaces used in the construction of dissimilar land cover types can be spectrally quite similar, this is especially the case of the slate and asphalt roofing materials when compared with that of the tarmac road surface. The Brown Cement roof tile exhibits a similar spectral response to soil, perhaps suggesting that distinguishing between this man-made roofing material and soil may prove problematic when using hyperspectral image data-sets.

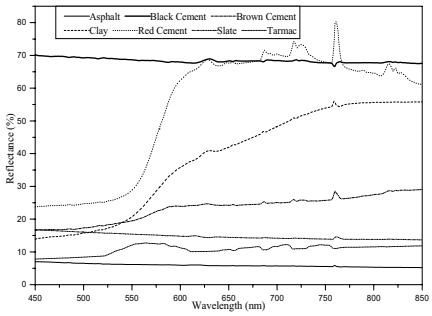

Figure 3. A plot of relative reflectance for all of the study surface materials from 300nm to 1000nm. The planimetric surface samples were recorded close to solar noon with a nadir-viewing angle. The solar zenith angle was 32^0 and the solar azimuth angle was 175^0.

3.2 *The broadband simulated reflectance of urban surface materials*

Table 2 shows the calculated broadband reflectance of the sample materials for the 4 spectral bands of the IKONOS multispectral sensor. In the case of each material, 10 reflectance measurements were used to calculate the mean band reflectance and corresponding standard deviation. Table 2 shows that the standard deviation for each of the samples is very small, showing little variance between the spectroscopy measurements taken in the field and therefore high sampling precision. As the means of the different materials exhibit little similarity for nearly all spectral bands of the IKONOS sensor, it would seem that one might expect on the basis of these values to be able to distinguish between these different materials at the broadband IKONOS multispectral level. It should be noted, however, that these measurements have been obtained in terms of the sample materials being placed in a planimetric (flat) manner and do not take into account 3-dimensional roof geometry.

Table 2. Surface material mean and standard deviation broadband reflectance values for each IKONOS band.

Surface	Blue		Green		Red		NIR	
	$\bar{x}$	σ	$\bar{x}$	σ	$\bar{x}$	σ	$\bar{x}$	σ
Asphalt	6	.03	6	.03	5	.03	5	.05
Black cement	66	.02	69	.04	63	.01	69	.03
Brown cement	16	.08	20	.08	23	.05	28	.06
Clay	15	.06	25	1.0	43	1.7	60	1.9
Red cement	23	.04	35	.06	63	.12	66	.18
Slate	16	.03	16	.30	13	.26	14	.29
Tarmac	8	.03	11	.01	10	.01	12	.01

3.3 *The angular reflectance of urban surface materials*

Figure 4 presents the results of measuring the reflectance of the sample materials for changes in viewing azimuth and zenith angle at $480\eta m$. This particular wavelength has been used in this case, because several of the sample materials exhibit similar reflectance at this wavelength when measured from nadir. Hence, an analysis of the angular reflectance characteristics of the materials at this wavelength will allow an initial judgement to be made on the potential to discriminate between spectrally overlapping man-made materials using angular samples of reflectance. Figure 4 shows, for several of the materials that exhibit spectral overlap in terms of their reflectance at $480\eta m$, that quite significant reflectance changes occur with respect to viewing azimuth and zenith. This is of interest when we compare these plots with that of the nadir plots in Figure 3. For instance, the tarmac road surface and the asphalt and slate roof surfaces show similar reflectance values at $480\eta m$ but distinctive viewing angle reflectance characteristics in Figure 4. Additionally the angular reflectance plots for the red cement; clay and brown cement samples also exhibit different patterns whereas their nadir reflectance values are broadly similar (Figure 3).

3.4 *Geometrical considerations for urban built form spectral reflectance.*

Figure 5(a) and 5(b) show the effect building roof geometry has on the reflectance of the man-made materials under investigation. In Figure 5(a) the reflectance values are recorded for increasingly zenith angles away from nadir (in the opposite direction to the incoming solar zenith angle) for a single gable-roof model. Figure 5(b) represents a similar angular sampling, but in this case for two gable-roof models, with reflectance being recorded for the model experiencing occlusion from direct solar illumination. In this instance the obstructed roof model shows a large decrease in reflectance for all of the sample wavelengths. This change in reflectance is in the order of a magnitude smaller than that of the directly

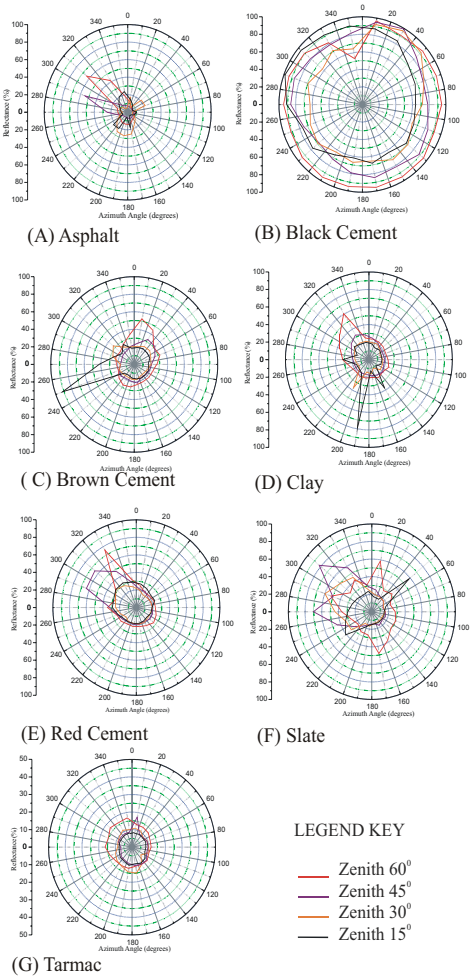

Figure 4. Polar co-ordinate plots of the relative reflectance value for each viewing azimuth and zenith for all samples at 480nm. Solar azimuth = 175^0, solar zenith = 32^0.

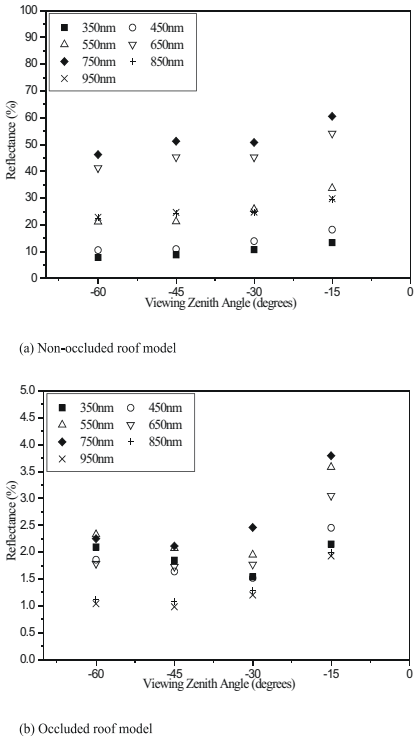

(a) Non-occluded roof model

(b) Occluded roof model

Figure 5. A plot of the reflectance spectra for a sample of wavelengths for the (a) non-occluded and (b) occluded roof models, where the principal plane of the roof faces run normal to that of the solar principal plane. Solar azimuth = 175^0, solar zenith = 32^0 for both scenarios. The occluded roof model results in (b) are scaled from 0 to 5% reflectance for clearer visual presentation.

illuminated roof (Figure 5a). This can be attributed to the obstructing neighbour impeding direct illumination and placing the roof in shadow.

When the results in Figures 5a and b are compared with that of the nadir planimetric reflectance of the sample materials in Figure 3, an interesting observation can be made. Under the planimetric scenario the red cement surface material shows a large difference in reflectance compared with that of the surface materials tarmac, slate and asphalt. In the obstructed roof model results of Figure 5b, the magnitude of reflectance is generally less than 5%. The difference between reflectance of the obstructed roof model and the planimetric tarmac, slate and asphalt samples has decreased significantly. This result suggests that the discrimination potential between the reflectance of sample materials would be decreased when they are measured under different geometric conditions.

4 DISCUSSION

The urban surface material samples investigated in this study show discriminatory capability both for the ground-based spectra and the converted broadband spectra. However, spatial heterogeneity of land cover and differences in irradiance conditions introduce difficulties in measuring reflectance at the satellite level (DeAbreau et al., 1994). Although the results we present here show that conversion from narrowband to broadband spectral resolution does not impede surface material discernability, the reflectance recorded by airborne or satellite sensors is affected by atmospheric attenuation, geometric dis-

tortion and sensor image resolution. For instance, the IFOV (instantaneous field of view) of the spectrometer fore optic used for this investigation was approximately 0.47m^2. The IFOV of a multispectral IKONOS image is, in comparison, 4m^2. At this spatial resolution individual pixel reflectance is more likely to be a composite of both building geometry effects and land cover mixing effects. This may produce a high degree of reflectance variance for resolved materials and hence limit their potential to be accurately derived using broadband multispectral Earth observation images.

The sample surface materials when measured through changing view angles exhibit different reflectance from that of their nadir response. The implication of this is that the addition of angular reflectance information could improve the discrimination between surface materials, especially where the reflectance between material types is similar or overlapping when measured from nadir. Future research will investigate the usefulness of angular information for urban surface material discrimination.

As the built structure of an urban area is not planimetric but constructed from a myriad of three dimensional roofs, this investigation has also attempted to provide some insight into the effect of building geometry on land cover inference. Most buildings, especially those with a residential land use, do not tend to appear in the landscape alone but are surrounded by other buildings, which can obstruct their direct solar illumination.

In this situation where a neighbour obstructs a roof from direct illumination, the resulting reflectance from the obstructed roof will be a construct of diffuse scattering from the surrounding buildings and indirect background scattering. In this study where the sensor is able to record a shadowed region, reflectance in the shaded area is strongly attenuated. The implication of this is that although there may be hyperspectral discriminatory potential between surface materials when sampled planimetrically; the realistic inclusion of urban geometry dampens reflectance in shadowed regions so strongly that confusion may be introduced between materials which previously had distinctive reflectance characteristics when their geometric situation was similar.

This feature may perhaps be a significant reason why accurate image classification of urban built forms has been unattainable, as recorded pixel response of a built-up area will be affected by a complex 3-dimensional built structure.

5 CONCLUSIONS

Overall, the results generated suggest that hyperspectral analysis may facilitate a good quantitative separation between certain built-form urban land cover types. However, for built-form land cover types of similar constituent materials (e.g., dark tarmac roads and dark asphalt roofs) angular reflectance characteristics may play a key role in statistically deriving separable spectral response patterns through the use of multiple view-angle measurements. Hyperspectral angular imaging is considered to have considerable potential for the recognition of urban surface materials. However, it should be taken into account that the geometrical effects of built-forms may result in spectral confusion between built-form land cover types thereby reducing class discrimination.

ACKNOWLEDGEMENTS

The authors would like to acknowledge the assistance of NERC's Equipment Pool for Field Spectroscopy for provision of the ASD Field SpecPro for a loan period in 2001 and for appropriate technical training in field spectroscopy, loan application 378.0701. The fieldwork could not have been completed without financial assistance from the School of Geography, University of Leeds.

REFERENCES

Ben-Dor, E., Levin, N., Saaroni, H., 2001. A spectral based recognition of the urban environment using the visible and near-infrared spectral region (0.4-1.1 μm). A case study over Tel-Aviv, Israel. *International Journal of Remote Sensing*, Vol. 22 (No. 11): 2193-2218.

DeAbreau, R.A., Keu, J., Maslinik, J., Serreze, M.C. & LeDrew, E.F., 1994. Comparison of in-situ and AVHRR-derived broadband albedo over Arctic sea ice. *Arctic*, Vol. 47: 288-297.

Ginneken, B.V., Stavridi, M., Koenderink, J.J., 1998. Diffuse and specular reflectance from rough surfaces. *Applied Optics*, Vol.37 (No.1): 130-139.

Heikkonen, J., Varfis, A., 1998. Land Cover/Land Use classification of Urban Areas: A Remote Sensing Approach. *International Journal of Pattern Recognition and Artificial Intelligence*, Vol.12 (No. 4): 475-489.

Nayar, S.K., Ikeuchi, K., Kanade, T., 1991. Surface reflection: physical and geometrical perspectives. *IEEE Transactions on Pattern Analysis and Machine Intelligence*, Vol.13: 611-634.

Price, C. J., 1995. Examples of high resolution visible to near-infrared reflectance spectra and a standardized collection for remote sensing studies. *International Journal of Remote Sensing*, Vol. 16 (No. 6): 993-1000.

Roessner, S., Segl, K., Heiden, U., et al. 2001. Automated differentiation of urban surfaces based on airborne hyperspectral imagery. *IEEE Transactions on Geoscience and Remote Sensing*, Vol. 39 (7): 1525-1532.

Sadler, G.J., Barnsley, M.J., & Barr, S.L., 1991. Information extraction from remotely sensed images for urban land-use analysis. In Proc: *Second European Conference on Geographical Information Systems (EGIS'91)*.

Smit, K. & Chandler, H.M. (Eds.), 1991. *Means Illustrated Construction Dictionary*. R.S. Means Company Incorporated, Kingston MA.

Space Imaging 2002. *IKONOS Relative Spectral Response and Radiometric Calibration Coefficients.* http://www.spaceimaging.com/aboutus/satellites/IKONOS/spectral.htm